Development 140, 4311-4322 (2013) doi:10.1242/dev.093922
© 2013. Published by The Company of Biologists Ltd

Atypical protein kinase C couples cell sorting with primitive endoderm maturation in the mouse blastocyst

Néstor Saiz*, Joanna B. Grabarek, Nitin Sabherwal, Nancy Papalopulu and Berenika Plusa‡

SUMMARY

During mouse pre-implantation development, extra-embryonic primitive endoderm (PrE) and pluripotent epiblast precursors are specified in the inner cell mass (ICM) of the early blastocyst in a 'salt and pepper' manner, and are subsequently sorted into two distinct layers. Positional cues provided by the blastocyst cavity are thought to be instrumental for cell sorting; however, the sequence of events and the mechanisms that control this segregation remain unknown. Here, we show that atypical protein kinase C (aPKC), a protein associated with apicobasal polarity, is specifically enriched in PrE precursors in the ICM prior to cell sorting and prior to overt signs of cell polarisation. aPKC adopts a polarised localisation in PrE cells only after they reach the blastocyst cavity and form a mature epithelium, in a process that is dependent on FGF signalling. To assess the role of aPKC in PrE formation, we interfered with its activity using either chemical inhibition or RNAi knockdown. We show that inhibition of aPKC from the mid blastocyst stage not only prevents sorting of PrE precursors into a polarised monolayer but concomitantly affects the maturation of PrE precursors. Our results suggest that the processes of PrE and epiblast segregation, and cell fate progression are interdependent, and place aPKC as a central player in the segregation of epiblast and PrE progenitors in the mouse blastocyst.

KEY WORDS: Lineage specification, Primitive endoderm, Epiblast, Mouse blastocyst, ICM, aPKC, GATA4, Pluripotency

INTRODUCTION

The development of the mammalian foetus is completely dependent on support from the extra-embryonic tissues, which provide the connection with the mother and are important signalling centres for patterning the early post-implantation embryo. The founder lineages for both the foetus and the extra-embryonic tissues arise sequentially from the totipotent blastomeres in the morula and early blastocyst. By the time of implantation, the blastocyst consists of three lineages: the extra-embryonic trophectoderm (TE) and primitive endoderm (PrE); and the epiblast, which develops into the foetus. The correct segregation of these three populations is therefore crucial, and failure to do so causes embryonic lethality. The formation of the TE has been studied extensively (reviewed by Cockburn and Rossant, 2010; Sasaki, 2010); however, the mechanisms regulating the segregation of the PrE and the pluripotent epiblast are only starting to be understood.

Epiblast and PrE are formed in a multi-step process from the inner cell mass (ICM) of the blastocyst (reviewed by Saiz and Plusa, 2013). In a first phase, epiblast and PrE precursors are specified in the naïve ICM of the early blastocyst (~32 cells). At this stage, all ICM cells express the epiblast markers *Nanog* and *Sox2*, and the early PrE markers *Gata6* and *Pdgfra* (Chazaud et al., 2006; Guo et al., 2010; Plusa et al., 2008). Several lines of evidence indicate FGF signalling is necessary for the specification of PrE cells (Arman et al., 1998; Feldman et al., 1995; Goldin and Papaioannou, 2003; Kang et al., 2013; Nichols et al., 2009; Yamanaka et al., 2010). Fgf4, which is produced by epiblast precursors, is thought to induce PrE fate among the rest of ICM cells (Frankenberg et al., 2011; Grabarek et al., 2012; Guo et al., 2010). Next, cell identity is reinforced, likely through sustained FGF signalling, leading to the exclusive expression of *Nanog* and *Gata6*/*Pdgfra* in epiblast and PrE precursors, which appear scattered in a 'salt and pepper' fashion in the mid blastocyst (~64 cells) (Chazaud et al., 2006; Plusa et al., 2008). PrE cells at this stage start to express GATA4 (Kurimoto et al., 2006; Plusa et al., 2008). Finally, from mid to late blastocyst (100-120 cells), these two lineages segregate into two separate compartments: PrE precursors migrate until they reach the surface of the ICM and become exposed to the blastocyst cavity, where they remain to eventually form a mature epithelium, leaving the epiblast enclosed between PrE and TE (Plusa et al., 2008). It has therefore been proposed that positional information is instrumental for the spatial segregation of PrE and epiblast (Gerbe et al., 2008; Plusa et al., 2008; Ralston and Rossant, 2008; Rossant, 1975). However, to date, no molecular players that translate positional information into the resolution of the 'salt and pepper' pattern have been identified. Furthermore, whether a relationship exists between the segregation of PrE and epiblast cells and lineage maturation has not been addressed.

Mature PrE cells become polarised, with receptors such as LRP2, or the endocytic adaptor DAB2, on their apical membrane (Gerbe et al., 2008; Yang et al., 2007) and the ability of PrE cells to become polarised has been proposed to be important for the sorting out of the PrE and epiblast (Moore et al., 2009; Rula et al., 2007). The atypical protein kinase C proteins (aPKCs) are involved in establishing apicobasal polarity and determining cell fate across metazoa (St Johnston and Ahringer, 2010). aPKCs are the most abundant of the PKC isoforms in the mouse pre-implantation embryo (Pauken and Capco, 2000) and play a central role in the polarisation of outer cells of the morula, which induces TE fate (Dard et al., 2009; Eckert et al., 2004a; Johnson and Ziomek, 1981; Plusa et al., 2005; Ralston and Rossant, 2008). We therefore sought to determine whether aPKC is involved in relaying positional

Faculty of Life Sciences, The University of Manchester, Oxford Road, Manchester M13 9PT, UK.

*Present address: Developmental Biology Program, Sloan-Kettering Institute, New York, NY 10065, USA
‡Author for correspondence (berenika.plusa@manchester.ac.uk)

This is an Open Access article distributed under the terms of the Creative Commons Attribution License (http://creativecommons.org/licenses/by/3.0), which permits unrestricted use, distribution and reproduction in any medium provided that the original work is properly attributed.

Accepted 5 August 2013

Development

signals that mediate the resolution of the 'salt and pepper' pattern and promote PrE maturation.

In this work, we present aPKC as a central player during the segregation of PrE and epiblast, where it couples cell sorting with lineage progression in PrE cells. We show that aPKC is enriched in prospective PrE cells prior to the sorting of the PrE and epiblast populations and prior to overt signs of cell polarisation. Subsequently, aPKC adopts a polarised localisation in PrE cells, only after they reach the blastocyst cavity and form a mature epithelium, in a process dependent on FGF signalling. We found that aPKC is necessary for PrE cell sorting and survival, and for its organisation as an epithelial layer. Moreover, inhibition of aPKC activity from the mid blastocyst stage not only prevents the sorting of PrE precursors into a polarised monolayer but concomitantly affects the maturation of PrE precursors. We propose a mechanism whereby aPKC translates positional information to resolve the 'salt and pepper' pattern by promoting both maturation of PrE and sorting of PrE and epiblast cells into separate layers.

MATERIALS AND METHODS

Embryo collection and culture

The mice used belonged to the CD1 strain, or the transgenic lines *Pdgfra*$^{H2B\text{-}GFP/+}$ (Hamilton et al., 2003), *CAG::GFP-GPI* (Rhee et al., 2006) or *CAG::H2B-EGFP* (Hadjantonakis and Papaioannou, 2004). Animals were maintained under a 12-hour light/dark cycle in the designated facilities of the University of Manchester, UK. Embryos from natural matings were collected and handled in M2 medium (Grabarek and Plusa, 2012) supplemented with 4 mg/ml BSA (Sigma) and staged as described previously (Plusa et al., 2008) (supplementary material Fig. S1A). Mouse handling and husbandry followed the regulations established in the UK Home Office's Animals (Scientific Procedures) Act 1986.

Embryos were cultured in microdrops of KSOM-AA medium (Grabarek and Plusa, 2012; Lawitts and Biggers, 1993) under mineral oil (Sigma) at 37.5°C in a 5% CO_2 atmosphere. The zona pellucida was always removed from embryos cultured from the early/mid blastocyst onwards by briefly washing in acidic Tyrode's solution (Sigma).

Inhibitors

All PKC inhibitors were purchased from Calbiochem (supplementary material Table S2). Increasing concentrations of the inhibitors were assayed (Table 2) and sublethal concentrations used to assess their effect on PrE organisation. The aPKC inhibitor Gö6983 was added to the culture medium at 5 μM for most experiments (Tables 1, 2). However, we observed batch-to-batch variation in the potency of the inhibitor; therefore, concentrations ranging from 5 (Lot# D00140253) to 10 μM (Lot# D00120125) were used in a set of experiments.

FGF signalling modulation

ERK1/2 and GSK3 inhibitors (2i) [PD0325901 (1 μM) and Chir99021 (3 μM), respectively (Nichols et al., 2009)] were a kind gift from Jenny Nichols (Cambridge Stem Cell Institute, Cambridge, UK). Recombinant human FGF4 (rhFGF4, R&D Systems) was diluted at 500 ng/ml in KSOM-AA in the presence of 1 μg/ml of heparin (Sigma) as described previously (Yamanaka et al., 2010).

RNAi

Double-stranded RNA (dsRNA) molecules were synthesised using the MEGAscript RNAi Kit (Ambion) following the manufacturer's instructions. Template DNAs (~400 bp) were amplified by PCR from CDSs cloned into plasmid vectors. Templates to produce dsRNA against mCherry and GFP (dsCherry and dsGFP) were amplified using the following primers: 5′-TAATACGACTCACTATAGGGAGACCGACTACTTGAAGCTGTC-CTT-3′ and 5′-TAATACGACTCACTATAGGGAGAGTTCCACG-ATGGTGTAGTCCTC-3′ for dsCherry; and 5′-TAATACGACTC-ACTATAGGGAGAAGCTGACCCTGAAGTTCATCTG-3′ and 5′-TAATACGACTCACTATAGGGAGAGATCTTGAAGTTCACCTTGA-TGC-3′ for dsGFP. Templates for dsRNA against *Prkci* (PKCλ) and *Prkcz* (PKCζ) were amplified using the following primers: 5′-TAATACG-ACTCACTATAGGGAGAGACAAGTCCATTTACCGGAGAG-3′ and 5′-TAATACGACTCACTATAGGGAGACGAAATCCTGCAGACCTA-GACT-3′ for PKCλ; and 5′-TAATACGACTCACTATAGGGAGATTTC-TTCATCTCGGAAACATGA-3′ and 5′-TAATACGACTCACTATAG-GGAGAGAAGTTTTCTCTGCCTCTGCAT-3′ for PKCζ.

All dsRNAs were diluted in nuclease-free water for injection. dsPKCs were injected at 250 or 500 ng/μl (for each isoform) in different experiments and dsCherry was injected at 500 ng or 1 μg/μl, respectively. The results with either concentration of dsPKCλ+ζ and dsCherry were equivalent, and therefore data from both concentrations were pooled together.

Synthetic mRNA preparation

All capped mRNAs were transcribed *in vitro* using the mMESSAGE mMachine kit (Ambion) following the manufacturer's recommendations. mRNAs were diluted in nuclease-free water and injected at 1 μg/μl.

Embryo microinjection

Single-blastomere injections were performed on glass depression slides (Fisher) on an inverted Leica DMI 6000B microscope equipped with DIC optics, Leica micromanipulators and an Eppendorf FemtoJet injector unit, essentially as described previously (Nagy et al., 2003) (see also supplementary material Fig. S2A).

Immunofluorescence

Embryos were fixed and immunofluorescence performed as described (Plusa et al., 2008). Details on the primary antibodies used are provided in supplementary material Table S1. All secondary antibodies were AlexaFluor (Invitrogen), diluted 1:500 and were applied for 60-75 minutes. Nuclei were stained with 5 μg/ml Hoechst 33342 (Sigma) in PBS.

Image acquisition

Four-dimensional (4D) imaging was performed in a Nikon A1R inverted confocal microscope equipped with an Okolab incubation chamber and a motorised stage for multi-point simultaneous imaging. Optical sections (2-3 μm) were taken every 15 minutes through whole embryos in order to build 3D *z*-stacks. Control and experimental embryos were imaged in parallel in each experiment and fixed at the end of the imaging period. *Z*-stacks of embryos injected with dsRNA were obtained at 24 hours post-injection (hpi) and subsequently fixed at 48 hpi. Fixed embryos were mounted in drops of ProLong Gold antifade reagent (Invitrogen) or directly in Hoechst solution on glass-bottom dishes (MatTek). Optical sections through fixed whole embryos were taken every 1-2 μm using an Olympus FluoView FV1000 inverted confocal microscope, a Nikon A1R or a Zeiss LSM 510 Meta.

Image analysis

Nuclei were manually counted using ImageJ (NIH) or Imaris (Bitplane). Movies were compiled from 4D sequences using Imaris. Immunofluorescence was quantified along linear regions of interest

Table 1. Embryo survival and PrE sorting

Treatment	Number of embryos	Survivors (%)	Dead (%)	Sorted (%)	Not sorted (%)	*P* value
1% DMSO	53	53 (100)	0 (0)	47 (88.7)	6 (11.3)	
5 μM Gö6983	58	57 (98.3)	1 (0.7)	20 (35.1)	37 (64.9)	<0.0001

Numbers (and proportions) of embryos that survived each treatment and that displayed a sorted PrE layer on the ICM surface. The difference in the number of sorted embryos between control and experimental embryos is highly significant (*P*<0.0001, two-tailed Fisher's exact test).

Development

Table 2. Screen for PKC inhibitors

Treatment	Number of embryos	Survivors (%)	Dead (%)	Number analysed	Sorted (%)	Not sorted (%)	*P* value
KSOM	28	28 (100)	0 (0)	28	22 (78.6)	6 (21.4)	
1% DMSO	37	37 (100)	0 (0)	32	25 (78.1)	7 (21.9)	
5 μM Gö6983	7	7 (100)	0 (0)	7	3 (42.9)	4 (57.1)	
10 μM Gö6983	30	30 (100)	0 (0)	25	10 (40)	15 (60)	<0.0001
20 μM Gö6983	8	0 (0)	8 (100)	0			
10 μM Gö6976	8	8 (100)	0 (0)	8	8 (100)	0 (0)	
20 μM Gö6976	19	6 (31.6)	13 (68.4)	0			
2.2 μM Rottlerin	7	7 (100)	0 (0)	1	1 (100)	0 (0)	
2.5 μM Rottlerin	34	15 (44.1)	19 (55.9)	14	11 (78.6)	3 (21.4)	
5 μM Rottlerin	6	1 (16.7)	5 (83.3)	0			
2 μM RO-31-8220	13	13 (100)	0 (0)	10	9 (90)	1 (10)	
2.5 μM RO-31-8220	14	8 (57.1)	6 (42.9)	7	6 (85.7)	1 (14.3)	
5 μM RO-31-8220	18	1 (5.6)	17 (94.4)	0			

Numbers of embryos (and proportions) that survived the treatment with increasing concentrations of broad-range PKC inhibitors and numbers of embryos that displayed a sorted PrE layer on the ICM surface. χ^2 analysis revealed a significant difference in the number of sorted embryos between the groups (P=0.0123). Comparison between groups revealed this difference was solely due to the numbers for sorted embryos treated with Gö6983, which show a highly significant difference from controls and from the rest of the inhibitors (P<0.0001). No significant difference between groups was found when Gö6983 embryos were excluded from the analysis.

(ROIs) using ImageJ. Linear ROIs minimise the bias when determining the limits of the region to be analysed (cell borders, in the absence of a membrane marker, and the breadth of the apical side), provide a large enough dataset and allow for a graphical representation of the protein distribution. ROIs were drawn across mid-sections of either single cells or groups of cells from the same lineage (Fig. 1B-D′) or along the apical or basolateral surfaces of cells lining the ICM surface (Fig. 1D″,G). Grayscale values for each ROI were averaged to obtain the mean intensity for each population and stage. At least four embryos were analysed per stage, with ROIs defined in three medial optical sections per ICM. Measurements were taken within the same or adjacent sections in order to avoid differences in intensity due to loss of signal along the *z* axis.

Embryos injected with dsRNA were analysed using ImageJ (NIH) and Imaris (Bitplane). Cell borders were marked by membrane-anchored GFP-GPI in *CAG::GFP-GPI* embryos (Rhee et al., 2006), which was used to score the position of labelled (H2B-GFP+) cells (inside or outside) at 24 hours on 3D stacks (see Fig. 3A).

Cell position was also scored on fixed embryos. Cells on the periphery of the blastocyst were scored as TE. We observed that the H2B-GFP signal often became too weak to be detected after fixation and immunofluorescence, making cell counting and scoring position challenging. In embryos injected with dsPKCλ+ζ, often a reduction in aPKC levels was evident, regardless of the presence of H2B-GFP (see Fig. 3G,H). In these cases, those cells were considered part of the injected clone. Whenever aPKC levels were simply lower than in neighbouring cells, or the difference was unclear, only the presence of H2B-GFP was used to determine the injected clone. In embryos injected with dsCherry, only the presence of H2B-GFP could be used to determine the progeny of injected cells, as aPKC levels were unaffected (Fig. 3F). Cells were scored as being on the ICM surface when one of their surfaces was exposed to the blastocyst cavity and as internal when completely surrounded by their neighbours. The presence or absence of GATA4 was scored for cells positioned either on the surface or the inside of the ICM.

Because of the different contribution to the ICM by control and experimental embryos in dsRNA experiments, the number of labelled cells in the ICM were normalised against the total number of labelled ICM cells for each embryo.

Statistical analysis

Statistical analyses were performed using Graphpad Prism. Statistical tests were performed as indicated in the text and figure legends. When applying the χ^2 test to analyse the effect of different inhibitors on PrE sorting, due to the low *n* values for some conditions, data for different concentrations of each inhibitor were pooled because there were no apparent differences between them (supplementary material Fig. S4B; Table 2).

RESULTS

aPKC is enriched in primitive endoderm precursors

The mature PrE in the peri-implantation blastocyst (E4.5) is an epithelium separating the epiblast from the blastocyst cavity (Dziadek and Timpl, 1985; Gerbe et al., 2008; Smyth et al., 1999). The localisation and role of the polarity protein aPKC have been well studied in the TE, the first extra-embryonic epithelium to form in the mouse (Dard et al., 2009; Pauken and Capco, 2000; Plusa et al., 2005), but not in the PrE. We therefore performed an immunolocalisation assay at consecutive stages of pre-implantation development in order to define the localisation pattern of aPKC in the PrE.

Up to the early blastocyst, aPKC presents high nuclear levels and localises to the cell contacts and the apical surface of outer cells, as previously described (Pauken and Capco, 2000; Plusa et al., 2005; Ralston and Rossant, 2008) (Fig. 1A). In the ICM of the early blastocyst, it is found throughout both cytoplasm and nuclei, as well as on cell contacts (Fig. 1A,E). In mid and late blastocysts (≈64-130 cells), aPKC levels are heterogeneous between individual ICM cells (Fig. 1A-C and supplementary material Movies 1, 2), with a distribution that resembles the ‘salt and pepper’ pattern of PrE and epiblast precursors (Chazaud et al., 2006) and suggesting aPKC could be marking one of these two populations. To examine this possibility, we co-stained embryos for aPKC and GATA4, a marker for PrE cells. GATA4 is found exclusively in PrE cells from the mid blastocyst onwards (Kurimoto et al., 2006; Plusa et al., 2008). High levels of aPKC are always found in cells positive for GATA4. Fluorescence intensity profiles through mid-sections of PrE (GATA4+) and epiblast (GATA4–) precursors revealed that PrE precursors in mid and late blastocysts are significantly enriched in aPKC compared with epiblast (Fig. 1B,C, charts; P<0.0001, n=15 sections in five embryos for mid blastocysts, n=18 sections in six embryos for late blastocysts). Cells negative for GATA4 were positive for NANOG (supplementary material Fig. S1C), as previously shown (Kurimoto et al., 2006; Plusa et al., 2008).

In E4.5 blastocysts, where all PrE cells are sorted into an epithelium on the ICM surface, aPKC localises to the apical membrane of PrE cells, presenting low cytoplasmic levels, equivalent to those of epiblast cells (Fig. 1D,D″,F,G). aPKC colocalises with other polarised components of the PrE, such as DAB2 (Gerbe et al., 2008) (Fig. 1G), although it seems to begin to polarise prior to DAB2 (supplementary material Fig. S1D).

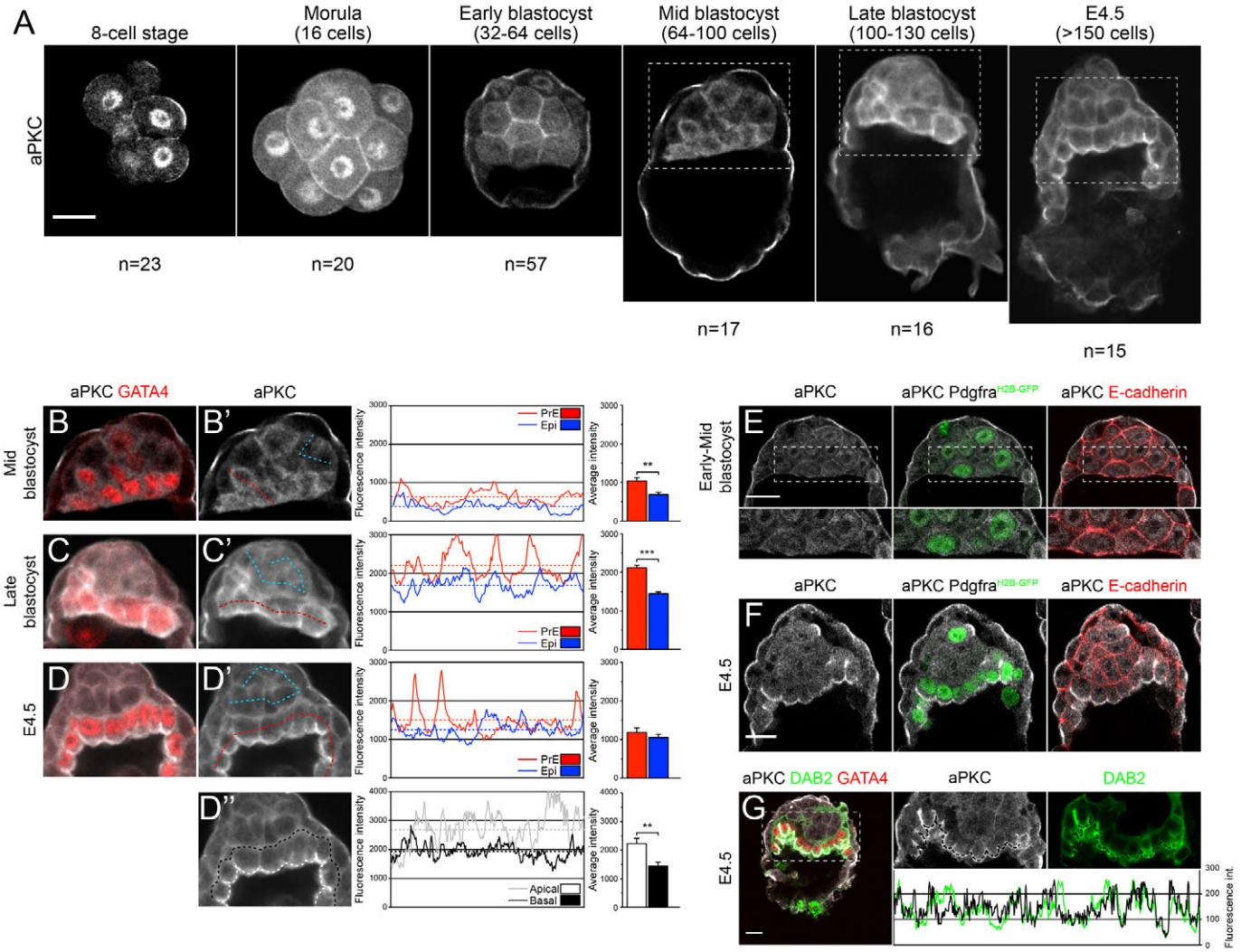

Fig. 1. aPKC is enriched in PrE precursors from the mid blastocyst. (**A**) Immunofluorescence for aPKC at successive stages of pre-implantation development. (**B-D′**) Quantification of aPKC levels from mid- to E4.5 blastocysts. Red lines/bars indicate PrE precursors (GATA4+); blue lines/bars indicate epiblast precursors (GATA4–). (**D″**) Quantification of aPKC levels along apical (grey/white) and basal (black) membranes of the PrE at E4.5. Histograms compare fluorescence intensity between both ROIs on the ICM depicted. Bar charts compare averages from several measurements. Dashed lines on histograms represent averages for profiles shown. (**E**) Immunofluorescence for aPKC and E-cadherin on an early-mid blastocyst showing aPKC localisation on the membrane/cortex. (**F**) Immunofluorescence for aPKC and E-cadherin at E4.5. There is a low aPKC staining throughout the ICM, except on the apical membrane of PrE cells. (**G**) Colocalisation of aPKC and DAB2 at E4.5. Histogram shows overlay of aPKC and DAB2 levels on the pictures above. $^{**}P<0.01$, $^{***}P<0.001$, unpaired Student's *t*-test. Bar charts display mean+s.e.m. *n*, number of embryos. Scale bars: 20 μm.

In summary, the distribution of aPKC in the ICM of the mouse blastocyst displays distinct phases that correlate with phases of PrE specification. Initially homogeneous levels of aPKC in the ICM of the early blastocyst become heterogeneous as embryos progress towards the mid blastocyst stage. aPKC thus becomes enriched in PrE precursors concomitantly with the establishment of the 'salt and pepper' pattern of PrE and epiblast precursors, prior to cell sorting. Finally, aPKC polarises in the mature, committed PrE epithelium. This correlation between the enrichment of aPKC and the specification of PrE precursors raises the issue of whether these processes are connected.

aPKC enrichment is specific to the primitive endoderm and depends on FGF/ERK signalling

To address whether the heterogeneity in aPKC levels throughout the ICM was a consequence of the acquisition of PrE fate, we prevented PrE specification by blocking ERK activity (Nichols et al., 2009; Yamanaka et al., 2010) and then assessed aPKC localisation.

We applied ERK1/2 and GSK3 inhibitors (2i) to embryos from the eight-cell stage to prevent PrE specification (Fig. 2A). Embryos cultured in the presence of 2i do not have PrE cells (marked by GATA4), as described (Fig. 2B,F) (Nichols et al., 2009). After 48 hours of culture in 2i (late blastocysts), embryos present homogeneous, low levels of aPKC throughout the ICM (Fig. 2F), whereas control embryos display significantly higher levels of aPKC in PrE cells, like late blastocysts (Fig. 2E, Fig. 1C; data not shown). After 72 hours in culture, control embryos have a polarised PrE (20/20 embryos, at least eight polarised cells), equivalent to E4.5 blastocysts (Fig. 2C,G,H; Fig. 1D). However, most embryos (23/26) treated with 2i present few (less than eight cells) or no polarised cells in the ICM (Fig. 2C,H).

Development

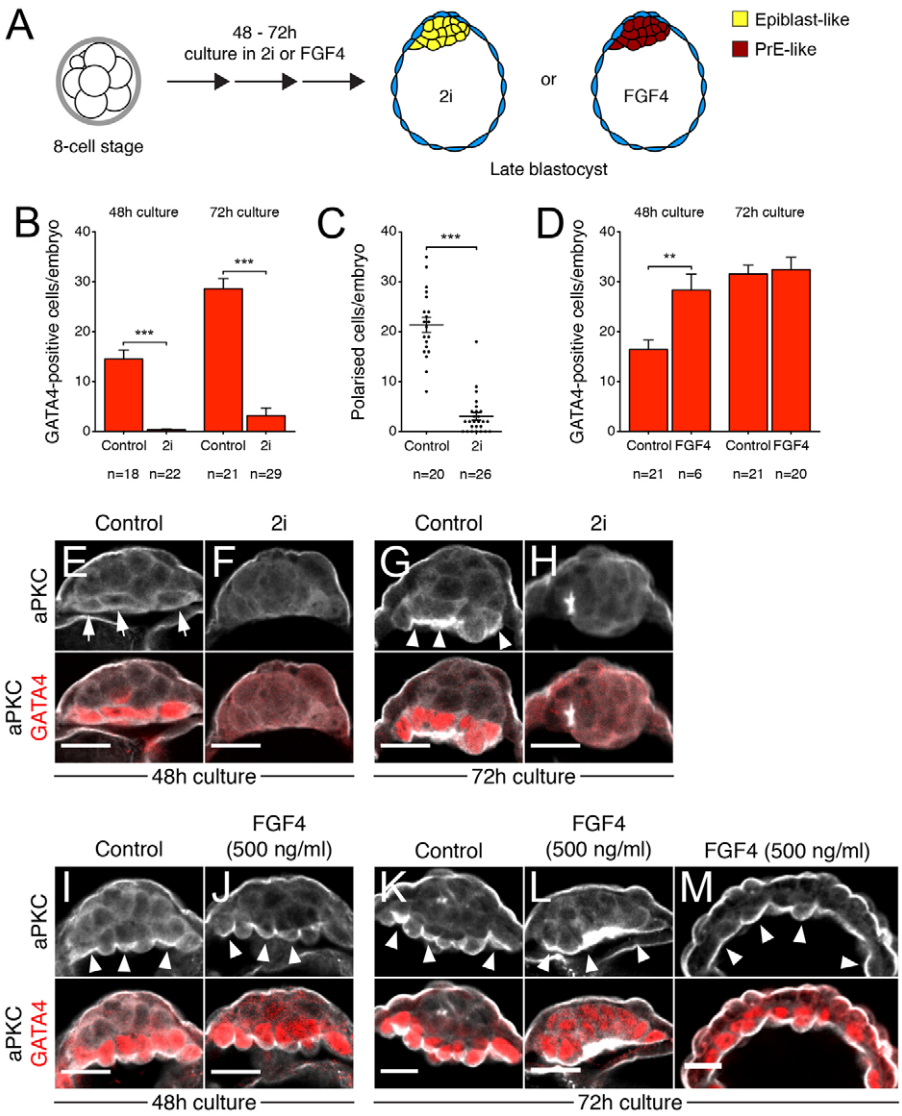

Fig. 2. aPKC enrichment and polarisation are downstream of FGF/ERK signalling.
(**A**) Schematic of 2i or Fgf4 treatment. (**B**) Number of GATA4 cells in control and 2i conditions. (**C**) Number of polarised cells on the ICM surface per embryo. 20/20 control embryos had at least eight cells. 23/26 2i-treated embryos had 0-6 polarised cells. (**D**) Number of GATA4 cells in control and Fgf4-treated embryos. (**E-H**) Immunofluorescence for aPKC and GATA4 in the ICM. (E) Higher levels of aPKC in PrE cells of control embryos after 48 hours (arrows), but not in those treated with 2i (F). (G) Polarised apical aPKC in PrE cells in controls after 72 hours (arrowheads), but not in 2i-treated embryos (H). (**I-M**) Immunofluorescence as in E-H for Fgf4 treatment. Both control (I,K) and experimental (J,L,M) embryos have apical aPKC in cells on the ICM surface (arrowheads). All data are collected from three replicas of each experiment. $^{**}P<0.01$, $^{***}P<0.001$, unpaired Student's *t*-test. Bar charts display mean+s.e.m. *n*, number of embryos. Scale bars: 20 µm.

We then cultured embryos in saturating doses of FGF4, which induce PrE fate throughout the ICM (Yamanaka et al., 2010). Embryos treated with 500 ng/ml of Fgf4 for 48 hours (Fig. 2A) express GATA4 throughout the ICM, and begin to show apically polarised aPKC in cells on the ICM surface, like control embryos cultured in parallel (Fig. 2D,I,J, arrowheads) (mean=16.4 GATA4+ cells, *n*=21 embryos in controls; mean=28.33 GATA4+ cells, *n*=6 in Fgf4-treated embryos). Interestingly, longer culture periods in Fgf4 (72 hours) do not result in a further expansion of the PrE when compared with controls, which also have an epiblast (mean=31.6 GATA4+ cells, *n*=21 embryos in controls; mean=32.5 GATA4+ cells, *n*=20 in Fgf4-treated embryos) (Fig. 2D). These data suggest FGF signalling is involved in the specification of the PrE, but is not sufficient for its proliferation. In embryos exposed to Fgf4 for 72 hours, although the entire ICM expresses GATA4, only ICM cells in contact with the cavity present aPKC on the apical membrane (Fig. 2K-M, arrowheads), indicating aPKC polarisation in PrE cells is dependent on cell position. Of note, however, in the majority of these embryos, the ICM becomes a monolayer, spread underneath the polar TE, with no epiblast (Fig. 2M). In these embryos, all ICM cells are polarised, indicating that aPKC polarisation is a hallmark of PrE epithelialisation.

These data show the heterogeneous levels of aPKC and its subsequent polarisation depend on the acquisition of PrE identity downstream of FGF signalling. Our results show the ability to develop an apical domain is inherent to PrE cells and dependent on both FGF/ERK signalling and cell positioning within the ICM. This ability may be essential for PrE organisation, as previously proposed (Moore et al., 2009; Rula et al., 2007).

Knockdown of aPKC prevents PrE cells from reaching the ICM surface

We have shown aPKC is specifically enriched in PrE precursors prior to cell sorting. To address the role of aPKC in PrE formation, we performed mosaic knockdown using double-stranded RNA (dsRNA)-mediated RNA interference (RNAi). dsRNA is highly efficient and specific for gene knockdown in pre-implantation embryos (Wianny and Zernicka-Goetz, 2000). In order to avoid defects in TE development as the result of aPKC knockdown in the whole embryo (Dard et al., 2009; Plusa et al., 2005), we targeted one single blastomere at the eight-cell stage, causing a mosaic knockdown (supplementary material Fig. S2A). As a technical control, we injected dsRNA against GFP (dsGFP), which was able to knock down efficiently GFP in *CAG::H2B-GFP; CAG::GFP-*

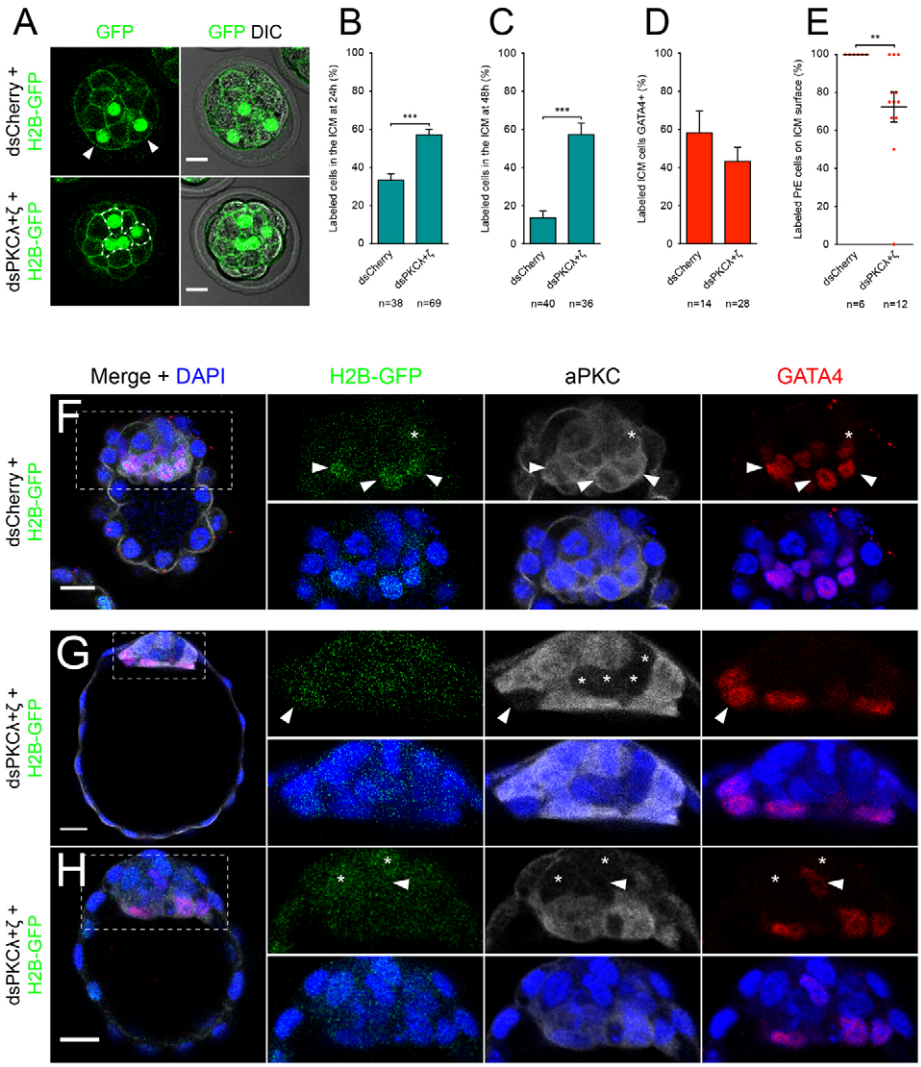

Fig. 3. Knockdown of aPKC prevents PrE cells from reaching the ICM surface. (**A**) Live images 24 hours post-injection (hpi). Arrowheads indicate cells on the ICM surface in control embryo. Dashed line indicates inner cells in experimental embryo. (**B**) Percentage of labelled ICM cells (H2B-GFP+) per embryo at 24 hpi. (**C**) Percentage of labelled ICM cells per embryo at 48 hpi. (**D**) Percentage of labelled PrE cells (GATA4+) per embryo at 48 hpi. (**E**) Percentage of labelled PrE cells (GATA4+) on the ICM surface per sorted embryo at 48 hpi. (**F-H**) Immunofluorescence for aPKC and GATA4 in representative embryos. Arrowheads indicate labelled GATA4+ cells. Asterisks indicate labelled GATA4– cells inside the ICM. Insets show the detail of ICMs. Each channel also overlaid with nuclear staining in all panels. $^{**}P<0.01$; $^{***}P<0.001$, unpaired Student's *t*-test (B,C) or Mann-Whitney U-test (D,E). Charts display mean+s.e.m. In scatter dot plot, each dot represents one embryo. *n*, number of embryos. Scale bars: 20 μm.

GPI embryos (Hadjantonakis and Papaioannou, 2004; Rhee et al., 2006) (supplementary material Fig. S2B).

Mouse pre-implantation embryos express both aPKC isoforms, PKCλ and PKCζ (Pauken and Capco, 2000). Therefore, we synthesised dsRNA molecules targeting both isoforms (dsPKCλ and dsPKCζ; see Materials and methods) that were co-injected with mRNA for H2B-GFP as a tracer. Control embryos were injected with dsRNA targeting mCherry. Consistently with previous reports, PKCλ+ζ knockdown causes an increased contribution to the ICM by the targeted cells compared to control embryos (Fig. 3A-C) (Dard et al., 2009; Plusa et al., 2005). No difference was found in the total number of labelled cells between controls and experimental embryos (supplementary material Fig. S2D,E). Furthermore, immunofluorescence at 24 hours post-injection (hpi) showed a marked reduction in cytoplasmic levels of aPKC (supplementary material Fig. S2C). Notably, nuclear aPKC is largely unaffected by the dsRNAs, suggesting this protein pool may be of maternal origin.

Embryos fixed at 48 hpi also display significantly more labelled cells in the ICM than control embryos (Fig. 3C). Therefore, for any further analysis of labelled ICM cells, numbers were normalised against the total number of labelled ICM cells for each embryo (in percent) (see Materials and methods for details). aPKC knockdown reduces the contribution to the PrE by the progeny of the injected cells, albeit not statistically significant (58.2% of GATA4+ labelled ICM cells for dsCherry, 43.2% for dsPKCs, $P=0.2526$ in Mann-Whitney U-test, Fig. 3D,F,G). However, in embryos injected with dsPKCs, there is a significant reduction in the proportion of labelled PrE cells (H2B-GFP+ and/or aPKC–, GATA4+) found on the ICM surface. All the labelled PrE cells were located on the ICM surface in control embryos, whereas only 72.4% of them were on the surface when aPKC was knocked down ($P<0.01$ in Mann-Whitney U-test) (Fig. 3E,F,H). In both cases, all non-labelled PrE cells in the embryos analysed were on the ICM surface.

Our data therefore show that in the absence of aPKC, PrE precursors fail to sort successfully, indicating aPKC may be necessary for the segregation of PrE and epiblast precursors.

Inhibition of aPKC in mid blastocysts impairs the segregation of PrE and epiblast

Our RNAi knockdown shows a defect in the sorting of PrE precursors in the absence of aPKC. However, it allows the analysis of only a subpopulation of cells. Therefore, we used an inhibitor to disturb aPKC throughout the embryo. This approach also allows temporal control of the treatment, so we applied the inhibitor to blastocysts over the time when the PrE and epiblast populations segregate (Fig. 4A).

We used the bisindolylmaleimide Gö6983 to inhibit aPKC. Bisindolylmaleimides are staurosporine derivatives with a higher

Development

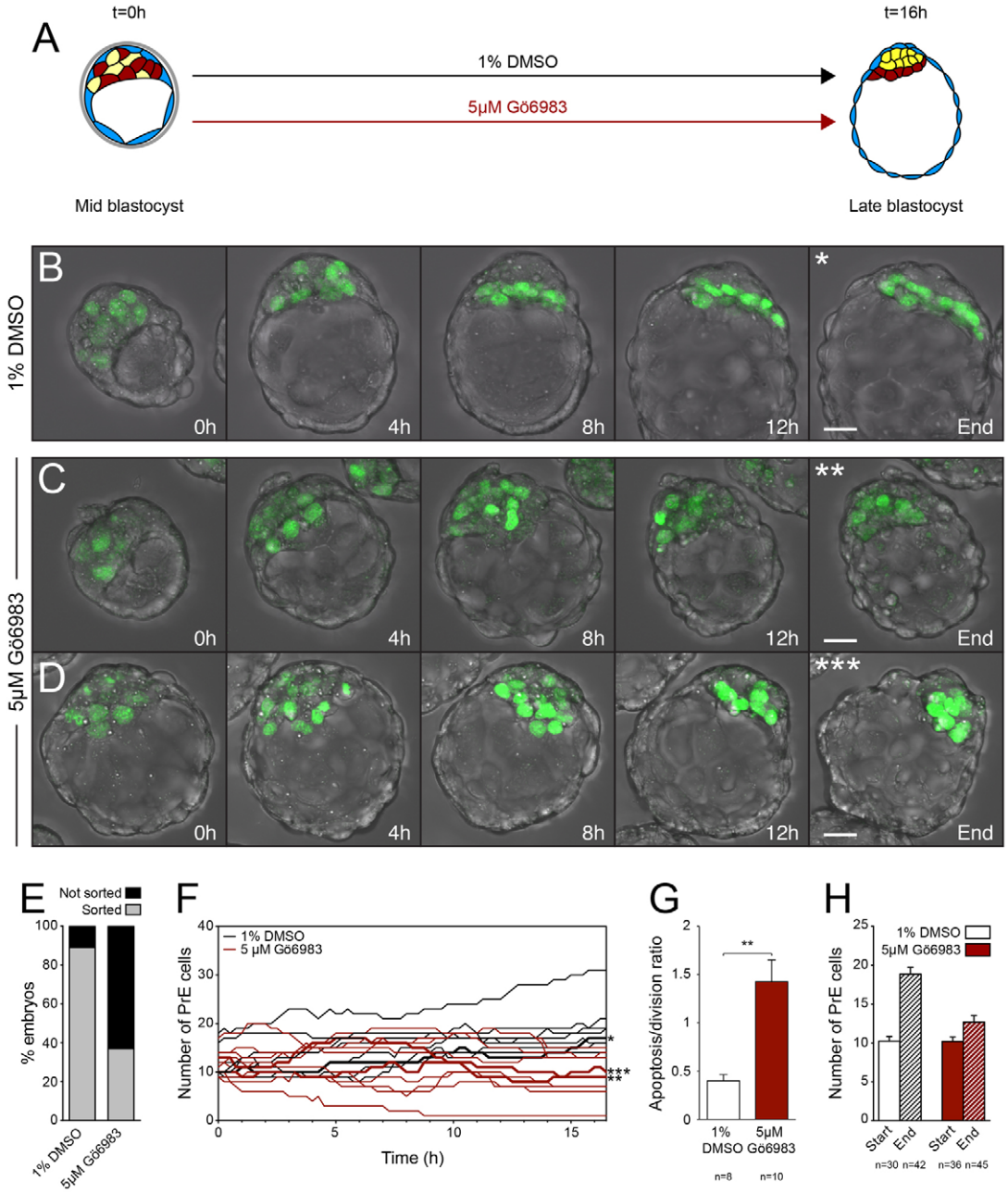

Fig. 4. Inhibition of aPKC in mid blastocysts impairs the segregation of PrE and epiblast. (**A**) Schematic of PKC inhibitor treatment. (**B**) Snapshots of a control embryo cultured in 1% DMSO. (**C**,**D**) Snapshots of two embryos cultured in 5 μM Gö6983. See supplementary material Movies 4-6, respectively. Green fluorescence indicates H2B-GFP expressed from the *Pdgfra* locus (PrE precursors). (**E**) Percentage of sorted embryos: 89% of embryos have a sorted PrE layer after 1% DMSO treatment, 37% of embryos have a sorted PrE layer after 5 μM Gö6983 treatment ($P<0.0001$, Fisher's exact test; see Table 1). (**F**) Time course of PrE expansion. Each line represents one embryo (number of GFP+ cells over time). Bold lines correspond to embryos in B-D as indicated (asterisks). (**G**) Number of apoptoses per cell division. (**H**) PrE (GFP+) expansion from the beginning to the end of the culture. $^{**}P<0.01$, unpaired Student's *t*-test. Bar charts display mean+s.e.m. Scale bars: 20 μm.

specificity for PKCs over other kinases (Gschwendt et al., 1995). This inhibitor has been used previously to show that aPKC is involved in TE formation (Eckert et al., 2004a) and can maintain ES cells in an undifferentiated state in the absence of LIF, through the inhibition of PKCζ (Dutta et al., 2011), suggesting it may prevent ICM differentiation. As a control for the activity of the inhibitor, we treated embryos with Gö6983 from the eight-cell stage up to the blastocyst stage. Treated morulas initiate cavitation but fail to expand the cavity and to maintain TE integrity (supplementary material Fig. S4A,B), consistent with the described role of aPKC in TE formation (Dard et al., 2009; Eckert et al., 2004b).

To gain more insight into the effect of blocking aPKC during PrE formation, we treated embryos with 5 μM of Gö6983 from the mid- to the late blastocyst, the period when PrE and epiblast precursors become segregated (Fig. 4A). We imaged this process using embryos that harbour a knock-in H2B-GFP fusion at the *Pdgfra* locus (*Pdgfra*$^{H2B\text{-}GFP}$), a bona fide reporter for *Pdgfra* expression,

which is a PrE marker (Hamilton et al., 2003; Plusa et al., 2008). Moreover, the presence of H2B-GFP in PrE cells allows visualisation of cell migration, cell division and cell death.

Live imaging of control embryos revealed PrE cells migrate throughout the ICM until they reach the surface, where they remain to form a layer between the epiblast and the blastocyst cavity (Fig. 4B and supplementary material Movie 4), as previously described (Plusa et al., 2008). However, in embryos treated with aPKC inhibitor, PrE precursors fail to remain on the ICM surface (Fig. 4B-D). They migrate through the ICM, but cannot maintain their position when they come into contact with the cavity. Instead, they often migrate deeper into the ICM, where they remain scattered or die by apoptosis (supplementary material Movies 5, 6). While 88.7% of control embryos (47/53) presented a sorted PrE layer at the end of the experiment, only 37% (20/54) of embryos treated with Gö6983 did (Fig. 4E; Table 1), a difference that was highly significant ($P<0.0001$).

We then followed the growth of the PrE population, scoring cell divisions and cell deaths in a subset of embryos (Fig. 4F). aPKC inhibition does not prevent cell division (supplementary material Movies 5, 6); however, there is an increase in the apoptosis:cell-division ratio that affects the expansion of the PrE (Fig. 4G). On average, we found a twofold increase in the size of the PrE compartment in control embryos, but no significant expansion in experimental embryos (Fig. 4H).

Given that Gö6983 also targets other PKC isoforms besides aPKC (Dutta et al., 2011; Gschwendt et al., 1995) (see supplementary material Table S2), we repeated our assay with a panel of commercial broad-range PKC inhibitors targeting all other PKC isoforms affected by Gö6983, except aPKC, to control for its specificity (supplementary material Table S2). Neither of these inhibitors, even the structurally related bisindolylmaleimide Gö6976, caused a phenotype like that observed for Gö6983 (supplementary material Fig. S3A,B; Table 2). Embryos developed normally in the presence of any of these inhibitors and presented a sorted PrE, with no apparent reduction in the number of GATA4+ cells (supplementary material Fig. S3A; Table 2). These results, in combination with our RNAi data, strongly indicate the phenotype observed is specifically the result of aPKC inhibition.

Our results therefore show that aPKC inhibition affects the behaviour of PrE precursors, which fail to organise as a layer on the ICM surface and display increased apoptosis. Interestingly, they do not seem to undergo a switch in cell fate, as they do when treated with FGF/ERK inhibitors, as they maintain *Pdgfra* expression (reported by H2B-GFP) (Fig. 4B-D), indicating that aPKC and FGF signalling have distinct effects on PrE identity.

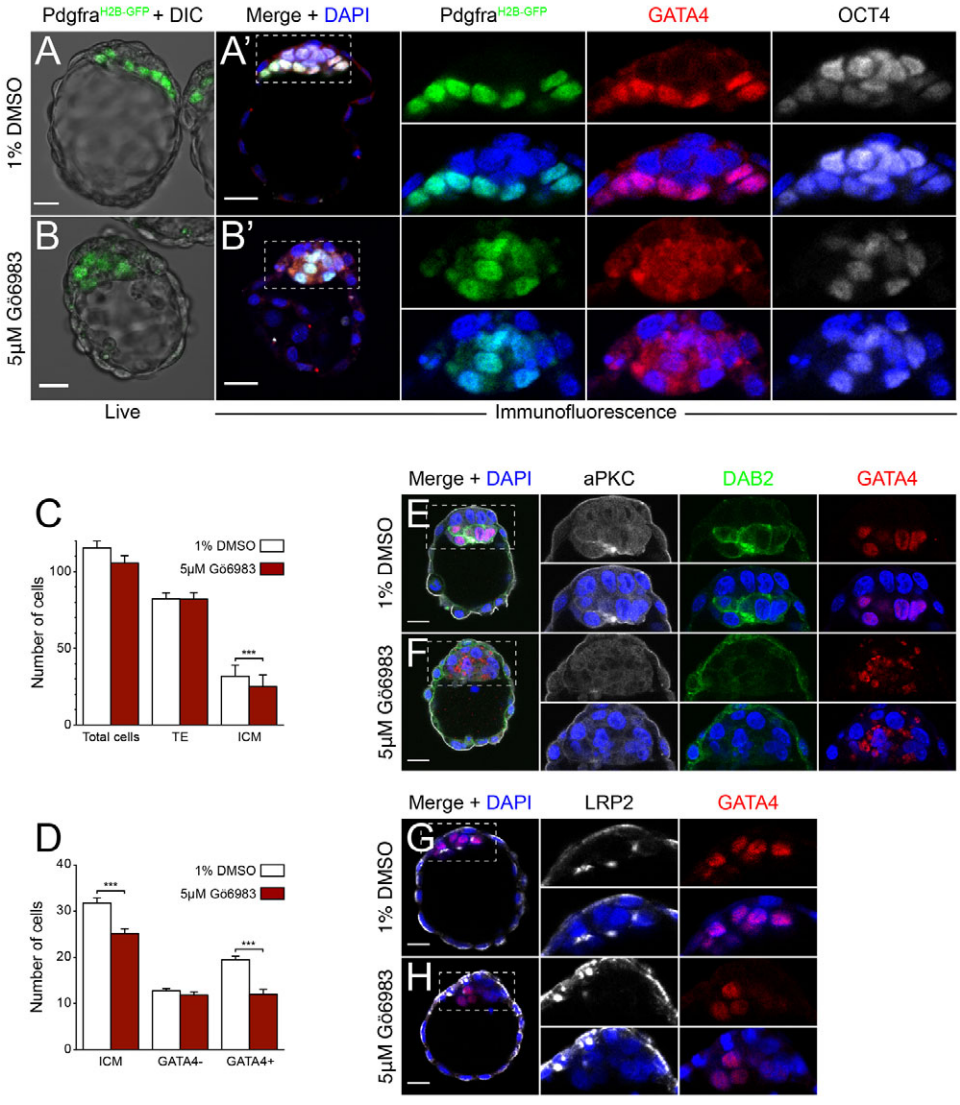

Fig. 5. Inhibition of aPKC prevents the maturation of PrE identity. (**A-B'**) Late blastocysts, live (A,B) and stained for GATAA4 and OCT4 after culture in 1% DMSO (A') or 5 μM Gö6983 (B'). GATA4 is present beyond the nuclear borders after treatment with Gö6983. See also supplementary material Movies 7-9. (**C**) Total, TE and ICM cell numbers. n=17 embryos for 1% DMSO, n=13 for 5 μM Gö6983. (**D**) Cell numbers for each ICM lineage. n=41 embryos for 1% DMSO, n=36 for 5 μM Gö6983. (**E-H**) Immunofluorescence for aPKC, DAB2 and GATA4 (E,F) or LRP2 and GATA4 (G,H). Insets show detail of ICMs. Each channel also overlaid with nuclear staining in all panels. ***$P<0.001$, unpaired Student's t-test. Bar charts display mean±s.e.m. Scale bars: 20 μm.

Development

Inhibition of aPKC prevents the maturation of PrE identity

We have shown that knockdown or inhibition of aPKC cause a defect in PrE sorting. However, the live reporter used allows visualisation of only PrE cells and changes in *Pdgfra* expression. To gain more insight into the state of ICM lineages upon aPKC inhibition, we analysed the expression of epiblast and PrE lineage markers in fixed samples.

Our live imaging data revealed a defect in the expansion of the PrE when embryos were treated with Gö6983, but did not show whether this was the result of a general increase in cell death throughout the embryo. OCT4 staining distinguishes ICM (OCT4+) from TE cells (OCT4–, in the periphery of the blastocyst). When combined with staining for GATA4 – the first exclusive marker of the PrE – it allows quantification of all three lineages in the blastocyst (PrE cells: OCT4+, GATA4+; epiblast cells: OCT4+, GATA4–) (see Fig. 5A′ and supplementary material Movie 7). We found no difference in the number of TE cells between control and experimental embryos (Fig. 5C), indicating aPKC inhibition does not affect the growth of the TE after this lineage has been established. However, treatment with Gö6983 causes a significant reduction in the number of ICM cells (Fig. 5C,D), which is entirely due to the observed reduction in the number of GATA4+ cells (Fig. 5D; Fig. 4H). By contrast, when embryos were allowed to develop in culture until an overt PrE layer was apparent on the ICM surface and then cultured for further 24 hours in the presence of the inhibitor (supplementary material Fig. S4C), no defect was observed in the PrE. Embryos grown in these conditions presented equivalent numbers of PrE cells as control embryos (supplementary material Fig. S4D; n=11 embryos for control group, n=8 for Gö6983). Moreover, they retained a monolayer of GATA4+ cells (supplementary material Fig. S4E,F), indicating that, as observed for the TE, aPKC activity is necessary for the establishment of the PrE epithelium, but not for maintaining the integrity of the mature tissue.

In addition, we found that embryos that cannot form a PrE layer concomitantly fail to develop a polarised apical surface. Control embryos display an apical domain of aPKC, LRP2 and DAB2 in PrE cells on the ICM surface, as described previously (Gerbe et al., 2008) (this report) (8/10 embryos for aPKC, 2/3 for DAB2, 3/5 for LRP2; Fig. 5E,G). However, most embryos treated with the inhibitor lack a polarised PrE (10/18 embryos for aPKC, 3/3 for DAB2, 11/13 for LRP2; Fig. 5F,H).

Both in control and experimental embryos, PrE cells maintain or upregulate *Pdgfra*$^{H2B\text{-}GFP}$ expression (Fig. 4B-D; supplementary material Movies 4-6), suggesting that aPKC inhibition does not cause a switch in cell fate. To test this hypothesis, we assessed the distribution of the epiblast marker NANOG and the PrE marker GATA4. We found the domains of NANOG and GATA4 expression do not overlap, in either control (8/8 embryos) or experimental embryos (8/8 embryos) (Fig. 6A,B), indicating there is no upregulation of epiblast markers in PrE precursors upon aPKC

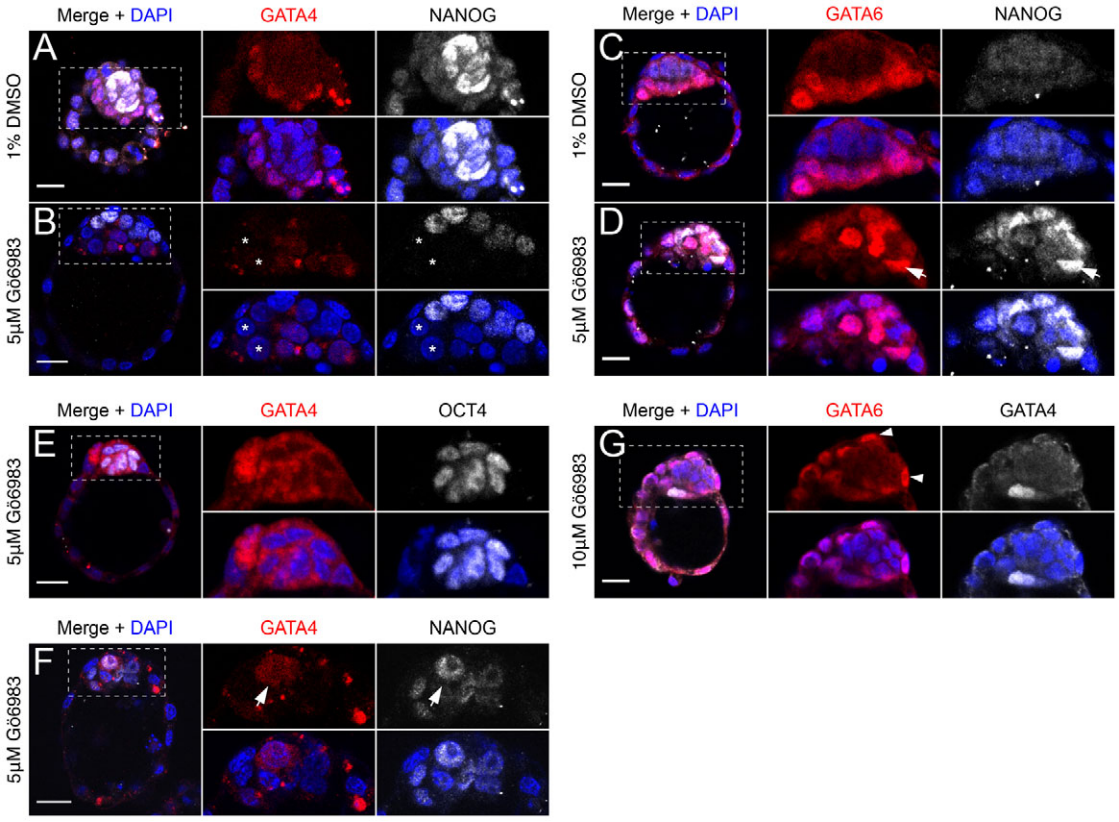

Fig. 6. Inhibition of aPKC prevents the maturation of PrE identity. (**A**,**B**) Immunofluorescence for GATA4 and NANOG in representative embryos after culture in 1% DMSO or 5 μM Gö6983. Asterisks indicate double-negative cells, with no staining for either NANOG or GATA4. (**C**,**D**) Immunofluorescence for GATA6 and NANOG as in A,B. Arrow indicates a NANOG+, GATA6+ cell on the ICM surface after Gö6983 treatment. (**E**) Immunofluorescence for GATA4 and OCT4 after treatment with 5 μM Gö6983. GATA4 is excluded from the nuclei present in the cytoplasm throughout the ICM. (**F**) Immunofluorescence for GATA4 and NANOG after treatment with 5 μM Gö6983. GATA4 is distributed throughout the cell marked with arrows (nucleus and cytoplasm). (**G**) Immunofluorescence for GATA4 and GATA6 after treatment with 10 μM Gö6983. Arrowheads indicate polar TE cells that retain GATA6 (normally found only in PrE and mural TE at this stage).

Development

inhibition. However, unlike control embryos, where all ICM cells are either NANOG+ or GATA4+ (7/8 embryos), all experimental embryos present between 1 and 3 double-negative cells (Fig. 6B, asterisks). These cells presumably express OCT4, as OCT4 is present in all ICM cells in equivalent assays, but they could not be assigned to either the epiblast or PrE lineage. Unexpectedly, GATA4 is often found in the cytoplasm upon aPKC inhibition (25/41 embryos, compared with 0/41 in controls) and occasionally completely excluded from the nucleus (Fig. 5B′; Fig. 6E,F; supplementary material Movie 8). However, we also found what seemed to be accumulations of the inhibitor in bright red speckles, making it hard to distinguish them from protein staining. These observations suggest aPKC inhibition may cause a loss of nuclear GATA4 in a proportion of PrE cells, which could account for the presence of NANOG–, GATA4– cells.

In order to test whether aPKC inhibition also affected the expression of earlier PrE markers, we stained embryos for NANOG and the early PrE marker GATA6. Unlike for GATA4, in these embryos we could never find double-negative cells (12/12 embryos treated with Gö6983, Fig. 6D), suggesting the NANOG–, GATA4– cells observed retain GATA6. Of note, GATA6 was never found to display cytoplasmic staining. Interestingly, although in control embryos the domains of NANOG and GATA6 never overlap (4/4 embryos) (Fig. 6C), 5/12 embryos treated with aPKC inhibitor displayed NANOG+, GATA6+ cells in the ICM (Fig. 6D, arrows). This result suggests inhibition of aPKC affects PrE maturation concomitant with its segregation and survival. To address this possibility, we double stained for GATA6 and GATA4. In all control embryos, GATA6 and GATA4 colocalise in PrE cells (3/3 embryos); however, we found that in 3/11 embryos treated with Gö6983, the domain of GATA6 expression was much broader than that of GATA4 (Fig. 6G).

These results indicate that, although aPKC inhibition does not cause a switch in cell fate from PrE to epiblast, it compromises the maturation of PrE cells. Moreover, the failure to segregate PrE and epiblast cells suggests the maturation of PrE cells could be linked to their organisation as a monolayer at the ICM surface. Interestingly, GATA4 has been previously proposed to be necessary for the correct spatial organisation of endoderm cells (Capo-chichi et al., 2005). This correlation suggests GATA4 might provide a link between cell sorting and lineage maturation in PrE cells.

DISCUSSION

In the ICM of the mammalian blastocyst, a stochastic gene expression pattern is gradually stabilised through paracrine stimulation of the FGF/ERK pathway to produce an ICM composed of intermingled PrE and epiblast precursors (Chazaud et al., 2006; Frankenberg et al., 2011; Kang et al., 2013; Nichols et al., 2009; Yamanaka et al., 2010). These two populations become separated into two compartments through active cell migration, anchoring of PrE cells at the ICM surface and elimination of mispositioned PrE cells (Meilhac et al., 2009; Plusa et al., 2008; Yamanaka et al., 2010). Although it has been proposed that polarisation of PrE cells may be important in this process (Gerbe et al., 2008; Moore et al., 2009; Rula et al., 2007), the molecular mechanisms driving it remain unknown. Here, we describe aPKC as a central player orchestrating the transition from the ‘salt and pepper’ distribution of PrE and epiblast cells into two separate mature lineages.

The distribution of aPKC in the ICM presents phases that correlate with phases of gene expression and changes in localisation of PrE cells, suggesting an involvement of aPKC in these processes. A specific increase in aPKC accompanies the specification of PrE cells and is maintained during PrE and epiblast segregation. aPKC only becomes polarised upon the establishment of the PrE as an epithelial monolayer, in the peri-implantation blastocyst (E4.5). Interestingly, it is at this stage that PrE and epiblast cells have been shown to be completely committed to their respective fates (Gardner and Rossant, 1979; Grabarek et al., 2012), indicating overt polarisation of aPKC is a hallmark of epithelialisation in the PrE and correlates with cell fate stabilisation.

We found that modulation of the FGF/ERK signalling pathway changes the levels and distribution of aPKC within the ICM. Our results not only show that aPKC is specifically enriched in PrE cells, but also that epiblast cells are unable to form an epithelium, even when engaged in asymmetrical cell contacts. The genetic programme triggered in PrE cells is thus very different from that of epiblast cells and directs the formation of a stereotypical, polarised epithelium with a basement membrane separating it from the epiblast (Dziadek and Timpl, 1985; Gerbe et al., 2008; Morrisey et al., 2000; Smyth et al., 1999; Yang et al., 2002). It does so partly in a cell-autonomous manner, as embryos treated with FGF4 lack an epiblast, but display a monolayer of polarised PrE cells. However, the epiblast may be necessary for proliferation of this tissue, because embryos grown with FGF4 have equivalent numbers of PrE cells to control embryos, which have an epiblast.

Importantly, we have shown that either knockdown or chemical inhibition of aPKC cause a defect in PrE sorting, as well as a marked increase in cell death among PrE cells. Apoptosis within the ICM has been previously described (Copp, 1978; Plusa et al., 2008) and it has been postulated as a mechanism to eliminate PrE cells mispositioned deep within the ICM (Plusa et al., 2008). Here, we show that when aPKC activity is blocked, PrE cells do not undergo cell fate switch – because they maintain the expression of early PrE markers – but do undergo apoptosis regardless of their location, suggesting they are unable to perceive positional cues, and therefore behave as mispositioned PrE cells.

Our results show that aPKC promotes survival and stabilises the position of PrE cells that reach the ICM surface before it becomes polarised. This suggests aPKC can affect cell fate independently of its role as a polarity protein. aPKC is known to regulate cell survival and apoptosis through the interaction with an array of signalling partners (Díaz-Meco et al., 1996; Leitges et al., 2001) (reviewed by Moscat et al., 2006; Puls et al., 1997; Sanz et al., 1999). Moreover, the role of nuclear aPKC described in other systems (Sabherwal et al., 2009) suggests nuclear aPKC in the blastocyst may be important in this process. The promiscuity of aPKC in its target selection and its ability to activate other transcription factors (Sanz et al., 1999; Sanz et al., 2000) makes it possible for it to directly or indirectly regulate GATA4 localisation in PrE cells. Although this possibility certainly requires more detailed investigation, our immunofluorescence data for GATA4 in conditions of aPKC inhibition suggest this could be the case. By contrast, we have not encountered cytoplasmic GATA4 when using RNAi, suggesting this could be either a non-specific effect of the inhibitor or the result of aPKC inhibition throughout the embryo instead of clonal downregulation. We show here that aPKC inhibition affects the maturation of PrE cells; in these conditions, cells can be found in the ICM that express OCT4 and GATA6, but not GATA4 (or NANOG), indicating that although these cells have adopted a PrE fate, they fail to progress further. Frankenberg and colleagues have shown that in the absence of NANOG and RTK stimulation, GATA6+ cells show increased cell death (Frankenberg et al., 2011). We speculate that in the absence of aPKC activity, cells that downregulate NANOG and maintain GATA6, but fail to activate GATA4, may

Development

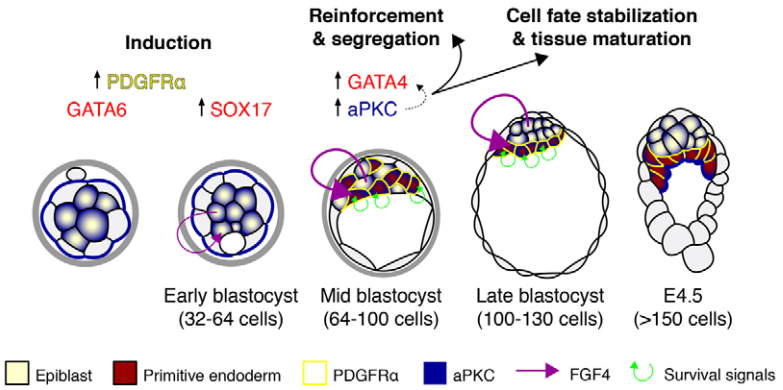

Fig. 7. Proposed model for PrE formation. ICM cells become primed towards a PrE or epiblast fate through the action of paracrine Fgf4. Sustained production of Fgf4 by epiblast precursors reinforces PrE fate, which is accompanied by aPKC enrichment in PrE precursors and upregulation of GATA4. aPKC would trigger survival signals in PrE cells that reach the ICM surface, which maintain their position. aPKC becomes polarised on the apical side of PrE cells at E4.5, when the PrE forms an epithelium.

also undergo cell death. This possibility could account for the low numbers of GATA6+, GATA4– cells found. The fact that *Gata4*$^{-/-}$ embryos survive until mid-gestation (Kuo et al., 1997; Molkentin et al., 1997) does not support this view; however, *in vitro* experiments using ES cells point in the same direction we propose (Capo-chichi et al., 2005; Soudais et al., 1995). Further details on the interaction between GATA6, GATA4 and other players (Capo-chichi et al., 2005) will be necessary before we can address this issue.

We therefore propose a model where aPKC couples the resolution of the 'salt and pepper' pattern of PrE and epiblast cells with the maturation of the PrE (Fig. 7). In this model, after an initial step of PrE specification mediated by FGF4, aPKC directs the sorting of PrE and epiblast cells into two distinct compartments, concomitantly with the maturation of lineage identities. Exposure of PrE cells to the blastocyst cavity would trigger survival signals in these cells, allowing the formation of a polarised epithelial layer and lineage commitment. Thus, our data imply that the sorting of PrE and epiblast cells represents the second major step in PrE formation, necessary for the transition from a primed to a mature state and where aPKC plays a pivotal role connecting cell sorting with progression of cell differentiation.

Acknowledgements
We thank Philippe Soriano for the *Pdgfra*$^{H2B-GFP}$ mice; Jenny Nichols for providing reagents, Kat Hadjantonakis and Josh Brickman for academic advice and support; and extensive input on this project; Chris Dee, Shane Herbert, the Papalopulu lab, Jenny Nichols, Alfonso Martínez Arias and Tilo Kunath for helpful comments and stimulating discussion; and the UoM BSU staff for animal husbandry.

Funding
N. Saiz was funded by Obra Social la Caixa and The University of Manchester. Work in N.P.'s lab is funded by a Wellcome Trust Senior Research Fellowship [090868/Z/09]. Work in B.P.'s lab is funded by a Manchester Fellowship and by the Biotechnology and Biological Sciences Research Council (BBSRC) [BP R107861]. Deposited in PMC for immediate release.

Competing interests statement
The authors declare no competing financial interests.

Author contributions
N. Saiz, B.P., N. Sabherwal and N.P. designed and discussed the experiments. N. Saiz and J.B.G. carried out the experiments. N. Saiz wrote the manuscript and assembled the figures. N. Saiz and B.P. edited the manuscript.

Supplementary material
Supplementary material available online at
http://dev.biologists.org/lookup/suppl/doi:10.1242/dev.093922/-/DC1

References

Arman, E., Haffner-Krausz, R., Chen, Y., Heath, J. K. and Lonai, P. (1998). Targeted disruption of fibroblast growth factor (FGF) receptor 2 suggests a role for FGF signaling in pregastrulation mammalian development. *Proc. Natl. Acad. Sci. USA* **95**, 5082-5087.
Capo-chichi, C. D., Rula, M. E., Smedberg, J. L., Vanderveer, L., Parmacek, M. S., Morrisey, E. E., Godwin, A. K. and Xu, X.-X. (2005). Perception of differentiation cues by GATA factors in primitive endoderm lineage determination of mouse embryonic stem cells. *Dev. Biol.* **286**, 574-586.
Chazaud, C., Yamanaka, Y., Pawson, T. and Rossant, J. (2006). Early lineage segregation between epiblast and primitive endoderm in mouse blastocysts through the Grb2-MAPK pathway. *Dev. Cell* **10**, 615-624.
Cockburn, K. and Rossant, J. (2010). Making the blastocyst: lessons from the mouse. *J. Clin. Invest.* **120**, 995-1003.
Copp, A. J. (1978). Interaction between inner cell mass and trophectoderm of the mouse blastocyst. I. A study of cellular proliferation. *J. Embryol. Exp. Morphol.* **48**, 109-125.
Dard, N., Le, T., Maro, B. and Louvet-Vallée, S. (2009). Inactivation of aPKClambda reveals a context dependent allocation of cell lineages in preimplantation mouse embryos. *PLoS ONE* **4**, e7117.
Díaz-Meco, M. T., Municio, M. M., Frutos, S., Sanchez, P., Lozano, J., Sanz, L. and Moscat, J. (1996). The product of par-4, a gene induced during apoptosis, interacts selectively with the atypical isoforms of protein kinase C. *Cell* **86**, 777-786.
Dutta, D., Ray, S., Home, P., Larson, M., Wolfe, M. W. and Paul, S. (2011). Self-renewal versus lineage commitment of embryonic stem cells: protein kinase C signaling shifts the balance. *Stem Cells* **29**, 618-628.
Dziadek, M. and Timpl, R. (1985). Expression of nidogen and laminin in basement membranes during mouse embryogenesis and in teratocarcinoma cells. *Dev. Biol.* **111**, 372-382.
Eckert, J. J., McCallum, A., Mears, A., Rumsby, M. G., Cameron, I. T. and Fleming, T. P. (2004a). PKC signalling regulates tight junction membrane assembly in the pre-implantation mouse embryo. *Reproduction* **127**, 653-667.
Eckert, J. J., McCallum, A., Mears, A., Rumsby, M. G., Cameron, I. T. and Fleming, T. P. (2004b). Specific PKC isoforms regulate blastocoel formation during mouse preimplantation development. *Dev. Biol.* **274**, 384-401.
Feldman, B., Poueymirou, W., Papaioannou, V. E., DeChiara, T. M. and Goldfarb, M. (1995). Requirement of FGF-4 for postimplantation mouse development. *Science* **267**, 246-249.
Frankenberg, S., Gerbe, F., Bessonnard, S., Belville, C., Pouchin, P., Bardot, O. and Chazaud, C. (2011). Primitive endoderm differentiates via a three-step mechanism involving Nanog and RTK signaling. *Dev. Cell* **21**, 1005-1013.
Gardner, R. L. and Rossant, J. (1979). Investigation of the fate of 4-5 day post-coitum mouse inner cell mass cells by blastocyst injection. *J. Embryol. Exp. Morphol.* **52**, 141-152.
Gerbe, F., Cox, B., Rossant, J. and Chazaud, C. (2008). Dynamic expression of Lrp2 pathway members reveals progressive epithelial differentiation of primitive endoderm in mouse blastocyst. *Dev. Biol.* **313**, 594-602.
Goldin, S. N. and Papaioannou, V. E. (2003). Paracrine action of FGF4 during periimplantation development maintains trophectoderm and primitive endoderm. *Genesis* **36**, 40-47.
Grabarek, J. B. and Plusa, B. (2012). Live imaging of primitive endoderm precursors in the mouse blastocyst. *Methods Mol. Biol.* **916**, 275-285.
Grabarek, J. B., Zyzyńska, K., Saiz, N., Piliszek, A., Frankenberg, S., Nichols, J., Hadjantonakis, A.-K. and Plusa, B. (2012). Differential plasticity of epiblast and primitive endoderm precursors within the ICM of the early mouse embryo. *Development* **139**, 129-139.
Gschwendt, M., Fürstenberger, G., Leibersperger, H., Kittstein, W., Lindner, D., Rudolph, C., Barth, H., Kleinschroth, J., Marmé, D., Schächtele, C. et al. (1995). Lack of an effect of novel inhibitors with high specificity for protein kinase C on the action of the phorbol ester 12-O-tetradecanoylphorbol-13-acetate on mouse skin in vivo. *Carcinogenesis* **16**, 107-111.

Guo, G., Huss, M., Tong, G. Q., Wang, C., Li Sun, L., Clarke, N. D. and Robson, P. (2010). Resolution of cell fate decisions revealed by single-cell gene expression analysis from zygote to blastocyst. *Dev. Cell* **18**, 675-685.
Hadjantonakis, A.-K. and Papaioannou, V. E. (2004). Dynamic in vivo imaging and cell tracking using a histone fluorescent protein fusion in mice. *BMC Biotechnol.* **4**, 33.
Hamilton, T. G., Klinghoffer, R. A., Corrin, P. D. and Soriano, P. (2003). Evolutionary divergence of platelet-derived growth factor alpha receptor signaling mechanisms. *Mol. Cell. Biol.* **23**, 4013-4025.
Johnson, M. H. and Ziomek, C. A. (1981). The foundation of two distinct cell lineages within the mouse morula. *Cell* **24**, 71-80.
Kang, M., Piliszek, A., Artus, J. and Hadjantonakis, A.-K. (2013). FGF4 is required for lineage restriction and salt-and-pepper distribution of primitive endoderm factors but not their initial expression in the mouse. *Development* **140**, 267-279.
Kuo, C. T., Morrisey, E. E., Anandappa, R., Sigrist, K., Lu, M. M., Parmacek, M. S., Soudais, C. and Leiden, J. M. (1997). GATA4 transcription factor is required for ventral morphogenesis and heart tube formation. *Genes Dev.* **11**, 1048-1060.
Kurimoto, K., Yabuta, Y., Ohinata, Y., Ono, Y., Uno, K. D., Yamada, R. G., Ueda, H. R. and Saitou, M. (2006). An improved single-cell cDNA amplification method for efficient high-density oligonucleotide microarray analysis. *Nucleic Acids Res.* **34**, e42.
Lawitts, J. A. and Biggers, J. D. (1993). Culture of preimplantation embryos. *Methods Enzymol.* **225**, 153-164.
Leitges, M., Sanz, L., Martin, P., Duran, A., Braun, U., García, J. F., Camacho, F., Diaz-Meco, M. T., Rennert, P. D. and Moscat, J. (2001). Targeted disruption of the zetaPKC gene results in the impairment of the NF-kappaB pathway. *Mol. Cell* **8**, 771-780.
Meilhac, S. M., Adams, R. J., Morris, S. A., Danckaert, A., Le Garrec, J.-F. and Zernicka-Goetz, M. (2009). Active cell movements coupled to positional induction are involved in lineage segregation in the mouse blastocyst. *Dev. Biol.* **331**, 210-221.
Molkentin, J. D., Lin, Q., Duncan, S. A. and Olson, E. N. (1997). Requirement of the transcription factor GATA4 for heart tube formation and ventral morphogenesis. *Genes Dev.* **11**, 1061-1072.
Moore, R., Cai, K. Q., Escudero, D. O. and Xu, X.-X. (2009). Cell adhesive affinity does not dictate primitive endoderm segregation and positioning during murine embryoid body formation. *Genesis* **47**, 579-589.
Morrisey, E. E., Musco, S., Chen, M. Y., Lu, M. M., Leiden, J. M. and Parmacek, M. S. (2000). The gene encoding the mitogen-responsive phosphoprotein Dab2 is differentially regulated by GATA-6 and GATA-4 in the visceral endoderm. *J. Biol. Chem.* **275**, 19949-19954.
Moscat, J., Rennert, P. and Diaz-Meco, M. T. (2006). PKCzeta at the crossroad of NF-kappaB and Jak1/Stat6 signaling pathways. *Cell Death Differ.* **13**, 702-711.
Nagy, A., Gertsenstein, M., Vintersten, K. and Behringer, R. (2003). *Manipulating the Mouse Embryo*, 3rd edn. New York, NY: Cold Spring Harbor Laboratory Press.
Nichols, J., Silva, J., Roode, M. and Smith, A. (2009). Suppression of Erk signalling promotes ground state pluripotency in the mouse embryo. *Development* **136**, 3215-3222.
Pauken, C. M. and Capco, D. G. (2000). The expression and stage-specific localization of protein kinase C isotypes during mouse preimplantation development. *Dev. Biol.* **223**, 411-421.
Plusa, B., Frankenberg, S., Chalmers, A., Hadjantonakis, A.-K., Moore, C. A., Papalopulu, N., Papaioannou, V. E., Glover, D. M. and Zernicka-Goetz, M. (2005). Downregulation of Par3 and aPKC function directs cells towards the ICM in the preimplantation mouse embryo. *J. Cell Sci.* **118**, 505-515.
Plusa, B., Piliszek, A., Frankenberg, S., Artus, J. and Hadjantonakis, A.-K. (2008). Distinct sequential cell behaviours direct primitive endoderm formation in the mouse blastocyst. *Development* **135**, 3081-3091.
Puls, A., Schmidt, S., Grawe, F. and Stabel, S. (1997). Interaction of protein kinase C zeta with ZIP, a novel protein kinase C-binding protein. *Proc. Natl. Acad. Sci. USA* **94**, 6191-6196.
Ralston, A. and Rossant, J. (2008). Cdx2 acts downstream of cell polarization to cell-autonomously promote trophectoderm fate in the early mouse embryo. *Dev. Biol.* **313**, 614-629.
Rhee, J. M., Pirity, M. K., Lackan, C. S., Long, J. Z., Kondoh, G., Takeda, J. and Hadjantonakis, A.-K. (2006). In vivo imaging and differential localization of lipid-modified GFP-variant fusions in embryonic stem cells and mice. *Genesis* **44**, 202-218.
Rossant, J. (1975). Investigation of the determinative state of the mouse inner cell mass. II. The fate of isolated inner cell masses transferred to the oviduct. *J. Embryol. Exp. Morphol.* **33**, 991-1001.
Rula, M. E., Cai, K. Q., Moore, R., Yang, D.-H., Staub, C. M., Capo-chichi, C. D., Jablonski, S. A., Howe, P. H., Smith, E. R. and Xu, X.-X. (2007). Cell autonomous sorting and surface positioning in the formation of primitive endoderm in embryoid bodies. *Genesis* **45**, 327-338.
Sabherwal, N., Tsutsui, A., Hodge, S., Wei, J., Chalmers, A. D. and Papalopulu, N. (2009). The apicobasal polarity kinase aPKC functions as a nuclear determinant and regulates cell proliferation and fate during Xenopus primary neurogenesis. *Development* **136**, 2767-2777.
Saiz, N. and Plusa, B. (2013). Early cell fate decisions in the mouse embryo. *Reproduction* **145**, R65-R80.
Sanz, L., Sanchez, P., Lallena, M. J., Diaz-Meco, M. T. and Moscat, J. (1999). The interaction of p62 with RIP links the atypical PKCs to NF-kappaB activation. *EMBO J.* **18**, 3044-3053.
Sanz, L., Diaz-Meco, M. T., Nakano, H. and Moscat, J. (2000). The atypical PKC-interacting protein p62 channels NF-kappaB activation by the IL-1-TRAF6 pathway. *EMBO J.* **19**, 1576-1586.
Sasaki, H. (2010). Mechanisms of trophectoderm fate specification in preimplantation mouse development. *Dev. Growth Differ.* **52**, 263-273.
Smyth, N., Vatansever, H. S., Murray, P., Meyer, M., Frie, C., Paulsson, M. and Edgar, D. (1999). Absence of basement membranes after targeting the LAMC1 gene results in embryonic lethality due to failure of endoderm differentiation. *J. Cell Biol.* **144**, 151-160.
Soudais, C., Bielinska, M., Heikinheimo, M., MacArthur, C. A., Narita, N., Saffitz, J. E., Simon, M. C., Leiden, J. M. and Wilson, D. B. (1995). Targeted mutagenesis of the transcription factor GATA-4 gene in mouse embryonic stem cells disrupts visceral endoderm differentiation in vitro. *Development* **121**, 3877-3888.
St Johnston, D. and Ahringer, J. (2010). Cell polarity in eggs and epithelia: parallels and diversity. *Cell* **141**, 757-774.
Wianny, F. and Zernicka-Goetz, M. (2000). Specific interference with gene function by double-stranded RNA in early mouse development. *Nat. Cell Biol.* **2**, 70-75.
Yamanaka, Y., Lanner, F. and Rossant, J. (2010). FGF signal-dependent segregation of primitive endoderm and epiblast in the mouse blastocyst. *Development* **137**, 715-724.
Yang, D. H., Smith, E. R., Roland, I. H., Sheng, Z., He, J., Martin, W. D., Hamilton, T. C., Lambeth, J. D. and Xu, X. X. (2002). Disabled-2 is essential for endodermal cell positioning and structure formation during mouse embryogenesis. *Dev. Biol.* **251**, 27-44.
Yang, D.-H., Cai, K. Q., Roland, I. H., Smith, E. R. and Xu, X.-X. (2007). Disabled-2 is an epithelial surface positioning gene. *J. Biol. Chem.* **282**, 13114-13122.